

Stereochemistry of Radical Halogenation Reactions. An ab Initio Molecular Orbital Study

Zhen-Hua Li,^{†,‡} Kang-Nian Fan,[‡] and Ming Wah Wong^{*,†}

Department of Chemistry, National University of Singapore, Kent Ridge Crescent, Singapore 119260, and Department of Chemistry, Fudan University, Shanghai 200433, China

Received: May 4, 2001; In Final Form: August 24, 2001

The stereochemistry of radical halogenation of alkyl halides has been studied by ab initio molecular orbital theory. Two key elementary reactions, hydrogen abstraction reaction [$\text{XCH}_2\text{CH}_3 + \text{Y}^\bullet \rightarrow \text{XCH}_2\text{CH}_2^\bullet + \text{HY}$ (**R1**)] and halogen abstraction reaction [$\text{XCH}_2\text{CH}_2^\bullet + \text{Y}_2 \rightarrow \text{XCH}_2\text{CH}_2\text{Y} + \text{Y}^\bullet$ (**R2**)], as well as rotational barrier of $\text{XCH}_2\text{CH}_2^\bullet$ radical, with $\text{X} = \text{H}, \text{F}, \text{Cl}$, and Br and $\text{Y} = \text{F}, \text{Cl}$, and Br , were studied using the G2(MP2,SVP) theory. Reactions **R1** and **R2** with $\text{X} = \text{F}, \text{Cl}$, and Br were found to be stereoselective. For $\text{X} = \text{F}$, both reactions prefer a gauche abstraction, whereas for $\text{X} = \text{Cl}$ and Br , both reactions prefer a trans pathway. The high rotational barriers of $\text{ClCH}_2\text{CH}_2^\bullet$ and $\text{BrCH}_2\text{CH}_2^\bullet$ radicals and the low abstraction barriers of their reactions with Cl_2 and Br_2 are the two main factors that guarantee the retention of their radical configuration during the abstraction reactions. Thus, radical chlorination and bromination of alkenes and chlorine- and bromine-substituted alkanes are predicted to be stereospecific, in good accord with experimental results. We show that the stereochemical control observed in radical halogenation reactions can be explained without the use of Skell hypothesis. The trends of the calculated energy differences between the gauche and trans transition states of reactions **R1** and **R2**, the rotational barriers of $\text{XCH}_2\text{CH}_2^\bullet$ radicals, and the gauche effect of XCH_2CH_3 can be rationalized in a uniform manner in terms of hyperconjugation interaction.

1. Introduction

In 1963, Skell et al. found that the free-radical bromination of optically active amyl bromide yields a single optical product, 1,2-dibromo-2-methylbutane,¹ whereas the bromination of (–)-1-fluoro-2-methylbutane yields a variety of reaction products.² The β -bromoethyl radical was then viewed as a (symmetrically or unsymmetrically) bridged structure in order to explain the stereochemistry in free-radical halogenation of alkanes and alkenes.^{2–4} However, several theoretical studies have shown that the β -bromoethyl radical has an open structure not bridged.^{5,6} Thus, the reason for retention of radical configuration in the radical bromination reactions remains an open question.

Free-radical halogenation is a very useful reaction to convert an alkane (RH) to an alkyl halide (RY). This type of radical reaction consists of four key steps: (a) generation of a halogen atom Y^\bullet (initiation step), (b) abstraction of a hydrogen atom of RH by Y^\bullet to generate a radical R^\bullet , (c) abstraction of a halogen atom of Y_2 by the R^\bullet radical to give the product RY, and (d) combination of two radicals, Y^\bullet and/or R^\bullet (chain termination step).

A graphical representation of the stereochemistry involved in the propagation steps b and c using the Newman projection is depicted in Figure 1. This schematic diagram illustrates that, in order to obtain stereospecific products for the radical halogenation of alkyl halides, three conditions must be fulfilled: (1) reaction b must be stereoselective, (2) the radical R^\bullet should retain its configuration during the hydrogen abstraction reaction, and (3) reaction c must be stereoselective. To maintain the configuration of the R^\bullet radical, two conditions must be

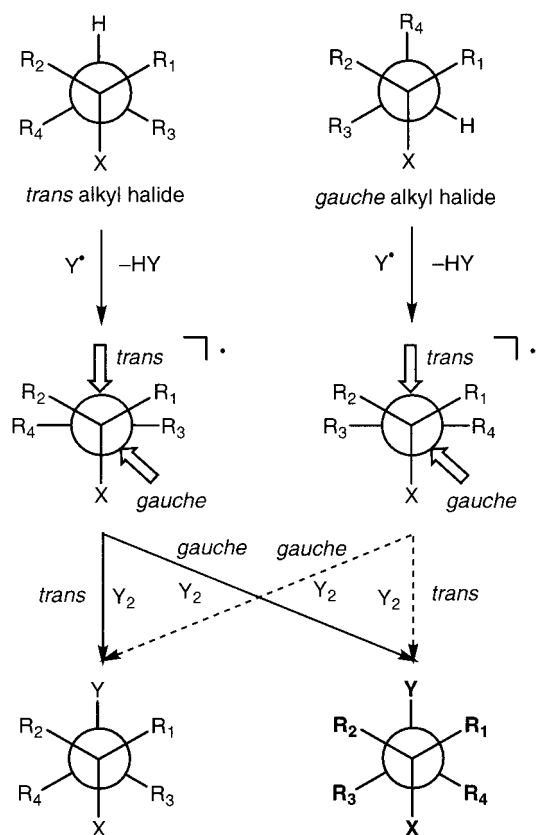


Figure 1. Schematic diagram for the radical halogenation (Y_2) of alkyl halide (RX) showing the different stereochemical products obtained by hydrogen abstracting at the trans and gauche positions.

satisfied: (i) the radical must have a relatively high rotational barrier and (ii) the energy barrier of step c should not exceed

* To whom correspondence should be addressed. Fax: (+65) 7791691. E-mail: chmwmw@nus.edu.sg.

[†] National University of Singapore.

[‡] Fudan University.

the rotational barrier of the radical. Free-radical halogenation of an alkene is similar to that of an alkane except for the second step; that is, the hydrogen abstraction is replaced by halogen addition to alkene.

To shed light on the stereochemistry of radical halogenation of alkanes and alkenes, we have investigated steps b and c of the radical fluorination, chlorination and bromination (i.e., Y = F, Cl, and Br) of the model system XCH₂CH₃ with X = H, F, Cl, and Br using the high-level G2(MP2,SVP) theory:



and



In addition, the rotational barriers of the intermediate XCH₂-CH₂[•] radicals have been examined. It is important to note that hydrogen abstraction from both α and β positions of alkyl halide (XCH₂CH₃) have been observed. In fact, α abstraction is observed to be slightly more favorable.²⁵ Our focus here is to investigate the reason for radical halogenation which produces stereoselective products at the β position. Hence, only β abstraction of reactions **R1** and **R2** is considered in this paper. Numerous theoretical studies have been reported on the structures, 1,2-migration barriers, rotational barriers of β -alkyl radicals,^{5–24,26} hydrogen abstraction reactions from haloethanes,^{25,27–29} and chlorination of haloethyl radicals,³⁰ but we are not aware of any theoretical studies on the gauche/trans selectivity of radical halogenation of alkanes and alkenes.

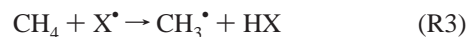
2. Computational Methods

All calculations in this work were carried out using the Gaussian 98³¹ suite of programs. The G2(MP2,SVP)³² theory was employed to examine the reaction profiles of the model reactions **R1** and **R2**. The transition states of both reactions were optimized for abstraction occurring at the gauche and trans positions relative to the X atom. The G2(MP2,SVP)³² method is a variant of the Gaussian-2 (G2)³³ theory. It requires two single-point energy calculations, QCISD(T)/6-31G(d) and MP2/6-311+G(3df,2p) at the MP2(full)/6-31G(d) optimized geometry. An effective energy at the QCISD(T)/6-311+G(3df,2p) level is obtained by applying the basis-set additivity assumption at the MP2 level. Zero-point energy (ZPE), calculated at the HF/6-31G(d) level and scaled by 0.8929, and the higher level correction (HLC) are added to the effective energy leading to an energy expression for the total energy at 0 K:

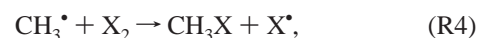
$$E_0 = E[\text{QCISD(T)/6-31G(d)}] + E[\text{MP2/6-311+G(3df,2p)}] - E[\text{MP2/6-31G(d)}] + \text{ZPE} + \text{HLC}$$

where $\text{HLC} = -An_\alpha - B(n_\alpha - n_\beta)$, with $A = 5.32$ and $B = 0.19$ mhartree. It is worth noting that the recently introduced G3(MP2)³⁴ method is a more accurate method than the G2(MP2,SVP) method and the calculations involved are essentially the same except for the use of a larger GTMP2Large basis set for the basis-set additivity calculation. Unfortunately, the GTMP2Large basis set is not currently available for bromine atom. Therefore, we have considered only the G2(MP2,SVP) method in this study. For the open-shell systems examined in this paper, calculations were carried out using an unrestricted (UHF) Hartree–Fock starting point.

In the standard G2(MP2,SVP) method, different levels of theory are used for geometry optimization and frequency calculation. Several theoretical studies have shown that it is better to use the same method for both geometry optimization and frequency calculation in studying a reaction profile.³⁵ In general, the geometry of a transition state is sensitive to the effect of electron correlation. Therefore, the HF method may even fail to locate the desired transition state in extreme cases. In the present study, we found that both the UHF and UB3-LYP³⁶ methods fail to locate the transition states for fluorine and bromine abstraction of CH₃[•] and XCH₂CH₂[•] radicals. Hence, we have employed the MP2(full)/6-31G(d) level for both geometry optimization and frequency computation for the G2(MP2,SVP) calculations carried out in this study. It is important to note also that the transition states for the halogen abstraction reactions considered here are highly spin-contaminated. In such cases, the MP2 geometries and frequencies may be erroneous.^{37,38} Thus, it is instructive to evaluate the reliability of the MP2(full)/6-31G* geometry and ZPE. To this end, we have studied the following two reactions (X = F, Cl, and Br)



and



with the G2(MP2,SVP) method, and compare the calculated energetics with results obtained with the higher-level CBS–RAD³⁸ method. Here, the CBS–RAD result is used as a benchmark, since this method has proven to be more reliable than the G2 types of methods for calculating thermochemical properties of radicals and studying radical reactions.^{38,39} Although the CBS–RAD method is very accurate, it is prohibitive and expensive for large systems, and it is not applicable for reactions involving bromine atoms, such as the reaction BrCH₂-CH₂[•] + Br₂.

For the CBS–RAD method employed in this study, the QCISD geometry optimization was carried out using the 6-31G(d,p) basis set, instead of 6-31G(d), because the 6-31G(d,p) basis set is a more balanced basis set for describing the hydrogen abstraction reactions. The ZPEs obtained at the MP2(full)/6-31G(d) and the QCISD/6-31G(d,p) levels were scaled by 0.9646 and 0.9776, respectively.⁴⁰ In the present study, it is the energy difference between the transition states, rather than the absolute value of the energy barrier, that is important. Thus, we have also applied the G2(MP2,SVP) and CBS–RAD methods to reactions **R1** and **R2** with X = Cl and Y = F and Cl to determine whether the calculated energy difference between the gauche and trans transition states is strongly influenced by the effect of geometry and the level of theory employed for calculating the energy barrier. Unless otherwise noted, calculated barriers and enthalpies reported in the text include ZPE correction.

3. Results and Discussion

3.1. Reactions R3 and R4. We begin our discussion by examining the structures and energetics of reactions **R3** and **R4** calculated using the G2(MP2,SVP) and CBS–RAD methods. For reaction **R3**, we found that the transition states obtained at the MP2/6-31G(d) and QCISD/6-31G(d,p) levels are similar (see the Supporting Information). Likewise, the choice of computational method has a small influence on the ZPE correction to energy barriers of reaction **R3**. On the other hand,

TABLE 1: Calculated Barriers and Enthalpies (kJ mol⁻¹) of Reactions R3 and R4 at Various Levels of Theory^a

X	$\langle S^2 \rangle^b$	barrier		enthalpy			
		G2(MP2,SVP)		G2(MP2,SVP)		CBS-RAD	
		MP2 ^c	QCISD ^d	MP2 ^c	QCISD ^d	QCISD ^d	
CH₄ + X[•](R3)							
F	0.77	2.4	2.9	-4.3	-121.3	-121.9	-120.7
Cl	0.78	32.5	32.7	25.3	23.4	23.4	23.7
Br	0.78	81.4	81.6		84.3	84.4	
CH₃[•] + X₂(R4)							
F	1.05	24.2	8.2	13.4	-332.4	-332.5	-322.5
Cl	0.88	-10.3	-7.2	-15.4	-128.7	-129.1	-122.3
Br	0.86	-11.8	-10.4		-110.0	-110.3	

^a Without ZPE correction. ^b The spin-squared expectation values ($\langle S^2 \rangle$, UHF/6-31G(d)) of the transition states. The $\langle S^2 \rangle$ values of CH₃[•], F[•], Cl[•], and Br[•] are 0.76, 0.75, 0.76, and 0.76, respectively. ^c MP2/6-31G(d) optimized geometries. ^d QCISD/6-31G(d,p) optimized geometries.

the level of theory used for geometry optimization and frequency calculation for reaction **R4** is very important, particularly for the fluorine abstraction (see the Supporting Information).

The activation barriers and reaction enthalpies calculated using the G2(MP2,SVP) and CBS-RAD methods are given in Table 1. All calculated energy values were obtained without the ZPE corrections. In general, the geometry optimization method has little effect on the reaction enthalpies of both reactions calculated with the G2(MP2,SVP) method. In addition, the reaction enthalpy of **R3** is not affected by the choice of energy calculation method. The difference between the values calculated with the two methods is small, only 0.3 and 1.3 kJ mol⁻¹ for X = Cl and F, respectively. On the other hand, the reaction enthalpy of reaction **R4** is greatly influenced by the choice of energy calculation method, where the G2(MP2,SVP) values are always too large by 7–10 kJ mol⁻¹.

The effect of geometry on the calculated barrier of reaction **R3** is small. The largest variation is only 0.5 kJ mol⁻¹. However, the magnitude of barrier is strongly dependent on the choice of the energy calculation method. The G2(MP2,SVP) barrier is consistently higher than the CBS-RAD value by about 7 kJ mol⁻¹. The choice of both geometry optimization level and energy calculation method has a large effect on the energy barrier of reaction **R4**. With the G2(MP2,SVP) method, the fluorine abstraction barrier at the MP2 geometry is too high by 16 kJ mol⁻¹, whereas chlorine and bromine abstraction barriers are too low, compared with values based on the QCISD geometry. Using the same QCISD geometries, the G2(MP2,SVP) barrier is too low by about 5 kJ mol⁻¹ for fluorine abstraction but too high by about 8 kJ mol⁻¹ for chlorine abstraction. The trend observed here is irregular. It is worth noting that the transition state of the most problematic case (X = F of reaction **R4**) is suffered from severe spin contamination ($\langle S^2 \rangle = 1.04$). Perhaps, this is the major cause of the problem in the UMP description of reaction **R4**. Although the energy difference between the gauche and trans transition states may be only several kJ mol⁻¹, the error associated with this method is of the same order of magnitude. On the basis of these results, it is clearly desirable to determine whether the relative energies between the gauche and trans transition states of reactions **R1** and **R2** can be predicted reliably by the G2(MP2,SVP) method.

3.2. Reactions R1 and R2 with X = Cl and Y = F and Cl. We have chosen X = Cl as a benchmark for reactions **R1** and **R2** because the effect of the Cl substituent on the energy barrier is expected to be in the middle of the series from X = F to Br. For economical consideration, only Y = F and Cl are consid-

ered. Here, the QCISD frequency was not calculated because ZPE difference between the gauche and trans transition states is expected to be small. As is evident in Table 2, the effect of geometry on the G2(MP2,SVP) energy difference is small. The energy difference calculated with the standard G2(MP2,SVP) method is close to that calculated using the CBS-RAD theory in all of the cases considered. This may be attributed to the fact that both the trans and gauche transition states have a similar $\langle S^2 \rangle$ value, which leads to a cancellation of errors. In fact, for all of the cases examined in this paper, the trans and gauche transition states are calculated to have an almost identical $\langle S^2 \rangle$ value (see subsequent sections). Thus, we are confident that the G2(MP2,SVP) method can provide reliable energy difference between the gauche and trans transition states, which is the primary interest in this study.

3.3. Hydrogen Abstraction Reaction R1 with X = H, F, Cl, Br and Y = F, Cl, and Br. The calculated barriers and reaction enthalpies of reaction **R1** are given in Table 3. The calculated reaction enthalpy increases on going from Y = F to Br. Hydrogen abstraction by fluorine atom is an exothermic reaction, whereas abstraction by bromine atom is predicted to be slightly endothermic. In the transition states of these hydrogen abstraction reactions, the forming and breaking bonds are roughly linear, i.e., C^{•••}H^{•••}Y is almost collinear. Because the reactants of both the gauche and trans abstractions are the same in reaction **R1**, the difference between the energy barriers of the gauche and trans abstraction (ΔE_a) is in fact the energy difference between the gauche and trans transition states. In this case, the ZPE difference between the gauche and trans transition states is small. Therefore, the difference between the energy barriers of the gauche and trans hydrogen abstraction can be attributed to the difference in the electronic structures of the two transition states.

Examination of Table 3 shows that ΔE_a increases from X = F to Br for any given Y. For X = F, the gauche transition state is always slightly lower in energy than the trans transition state (by 0.4–2.7 kJ mol⁻¹) and vice versa for X = Cl and Br. Except for the case of X = Cl and Y = Br, the absolute value $|\Delta E_a|$ increases on decreasing the halogen group for any given X. This clearly indicates that, as the abstraction barrier increases, i.e., as Y becomes less reactive, the reaction becomes more selective. This finding is, perhaps, not new for chemists. The main interest here is to understand why the ΔE_a value changes from a negative value to a large positive value on going from F to Br.

Several semiempirical methods have been proposed to predict the magnitude of hydrogen abstraction barriers.⁴¹ Most of these methods are based on properties of the reactants and products, such as bond energies, reaction enthalpies, electron affinities, and ionization potentials. These quantities are all the same for both trans and gauche abstraction pathways of reaction **R1**, and therefore, they are not site specific. Hence, these approaches cannot provide insight into factors governing the stereoselective behavior. Possible properties which are unique to reaction site are the atomic charge of hydrogen atom, and the bond order and bond length of the C–H bond of the reactant. A conceivable alternative approach to understand the stereochemistry is to analyze the geometry and electronic properties of the transition state involved.

To examine the atomic charges of the hydrogen atoms and the Wiberg bond order indices⁴² of the C–H bonds in the XCH₂-CH₃ reactant, we have performed the natural bond order (NBO)⁴³ analysis on the basis of the HF/6-31G(d) wave function. The calculated atomic charges and bond indices, together with the C–H bond lengths in XCH₂CH₃, are listed in

TABLE 2: Calculated Energy Differences^a (kJ mol⁻¹) between the gauche and trans Transition States for Reactions R1 and R2

reaction	$\langle S^2 \rangle^b$		G2(MP2,SVP)		CBS-RAD
	trans	gauche	MP2/6-31G(d) ^c	QCISD/6-31G(d,p) ^c	QCISD/6-31G(d,p) ^c
ClCH ₂ CH ₃ + F [•]	0.77	0.77	1.8	1.3	2.6
ClCH ₂ CH ₂ [•] + F ₂	1.04	1.04	6.2	6.5	7.3
ClCH ₂ CH ₃ + Cl [•]	0.78	0.78	4.7	6.8	4.8
ClCH ₂ CH ₂ [•] + Cl ₂	0.87	0.87	5.6	5.8	8.1

^a Without ZPE correction. ^b The spin-squared expectation values ($\langle S^2 \rangle$, UHF/6-31G(d)) of the transition states. ^c Level of geometry optimization.

TABLE 3: Calculated^a Barriers and Enthalpies (kJ mol⁻¹) of Reaction R1 (XCH₂CH₃ + Y[•] → XCH₂CH₂[•] + HY)

X	Y	barrier (E_a) ^b			ΔE_a ^c	enthalpy
		trans	gauche			
H	F	-16.1 (0.77)				-152.0
F	F	-10.4 (0.77)	-10.8 (0.77)	-0.4		-142.8
Cl	F	-13.5 (0.77)	-11.7 (0.77)	1.8		-148.6
Br	F	-14.1 (0.76)	-11.1 (0.76)	3.1		-155.3
H	Cl	-9.1 (0.78)				-13.2
F	Cl	7.6 (0.78)	5.4 (0.78)	-2.2		-3.9
Cl	Cl	-0.4 (0.78)	4.4 (0.78)	4.7		-9.8
Br	Cl	-4.9 (0.78)	3.7 (0.79)	8.6		-16.5
H	Br	40.6 (0.78)				45.7
F	Br	56.5 (0.78)	53.8 (0.78)	-2.7		55.0
Cl	Br	47.8 (0.78)	52.0 (0.78)	4.2		49.1
Br	Br	42.0 (0.78)	52.9 (0.79)	10.9		42.4

^a G2(MP2,SVP) values (include ZPE correction). ^b The (S^2) values of the transition states are given in parentheses. ^c Difference between the barriers of gauche and trans abstractions.

TABLE 4: Calculated Atomic Charges of Hydrogen Atoms, C–H Bond Lengths, and C–H Bond Orders of the gauche and trans Positions of the X Group in XCH₂CH₃

X	charge on hydrogen ^a		C–H bond length (Å) ^b		C–H bond order ^c	
	trans	gauche	trans	gauche	trans	gauche
H	0.213	0.213	1.093	1.093	0.942	0.942
F	0.220	0.226	1.093	1.092	0.936	0.934
Cl	0.225	0.230	1.094	1.091	0.929	0.934
Br	0.225	0.232	1.095	1.091	0.927	0.932

^a NBO analysis, based on HF/6-31G(d)//MP2/6-31G(d) wave function. ^b MP2/6-31G(d) geometries. ^c Wiberg bond order indices.

Table 4. As seen in this table, when X is a halogen atom, the hydrogen atoms at the reaction site are no longer equivalent. For instance, the H atom at the gauche position always carries a more positive charge than that at the trans position. Furthermore, the trans C–H bond is always shorter by 0.001–0.004 Å. The bond order analysis, however, shows a different trend compared with the trends of atomic charge and bond length. The C–H bond order at the trans position is larger than that at the gauche position for X = F but smaller for X = Cl and Br, indicating the C–H bond at the gauche position is weaker for X = F while stronger for X = Cl and Br. The C–H bond order at the trans position decreases from F to Br, whereas that at the gauche position remains almost the same. The trend in bond orders parallels the trend in energy barriers, where the gauche abstraction barrier for the same Y remains almost the same and the trans abstraction barrier decreases from F to Br for the same Y (Table 3). Thus, it seems that the C–H bond order is a better index than the calculated charge and bond length for indicating the reactivity of hydrogen abstraction.

Second-order perturbation analysis indicates that the strength of the hyperconjugation interaction between the C–X bond and the trans C–H bond in XCH₂CH₃ increases on decreasing the halogen group. The hyperconjugation interaction is mainly

attributed to a mixing between the C–H bonding orbital and the C–X antibonding orbital (σ^*), and the strength of this interaction increases from F to Br. Thus, hyperconjugation makes the C–H bond at the trans position weaker from F to Br. This explains why the trans C–H bond order decreases from F to Br, whereas the gauche C–H bond order remains the same (Table 4).

At the first sight, the use of bond order to explain the trend in the differences between the gauche and trans abstraction barriers is contradictory to the fact that energy barriers of R1 with X = F, Cl, and Br are higher than that with X = H, whereas the bond order of the C–H bond in XCH₂CH₃ with X = F, Cl, and Br is smaller than that with X = H. The increase of the energy barrier from X = H to X = F, Cl, and Br is due to the inductive effect of the electronegative halogen atom. This is reflected in the calculated atomic charges on the hydrogen atoms in XCH₂CH₃ (X = F, Cl, and Br), which are always smaller than those of the parent analogue (X = H). When calculating the energy difference between the gauche and trans transition states, this inductive effect is effectively canceled out.

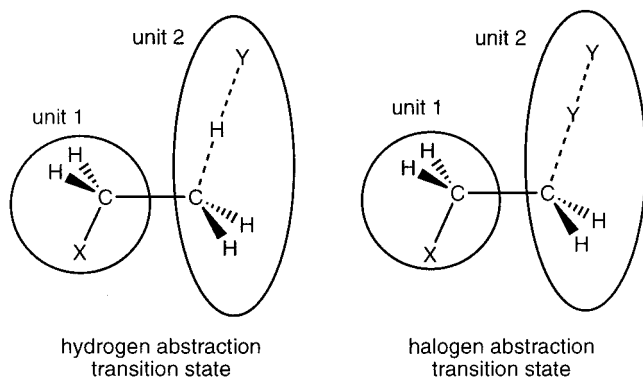
Plausible factors which may influence the magnitude of ΔE_a of reaction R1 include (1) polar effect, represents the dipole–dipole interaction between the bonds on the two carbon atoms, (2) steric effect, mainly the repulsion between X and Y atoms, and (3) stereoelectronic effects. The steric effect is expected to be small here because the X and Y atoms are far apart from each other. Therefore, only the dipole–dipole interaction and the stereoelectronic effect are likely to be important. The dipole–dipole interaction favors the trans transition state. Its contribution can be roughly indicated by the difference in dipole moment between the two transition states. In all cases, the dipole moment of the gauche transition state is always higher than that of the trans transition state, as indicated in Table 5. For Y = F and Br, the difference in dipole moment first decreases and then increases from F to Br, whereas the energy difference between the two transition states (ΔE_a) increases steadily on going from X = F to Br. This suggests that the dipole–dipole interaction is too weak to affect the sequence of the energy differences.

As with the XCH₂CH₃ reactant, one may employ a similar population analysis to examine the stereoelectronic effect in the transition state of reaction R1. Here, we have calculated the hyperconjugation contribution to the energy of the transition states (E_{hyper}) based on the NBO analysis. The E_{hyper} value is computed by deleting all of the possible delocalization interactions between the unit 1 and unit 2 of the transition state (Figure 2), i.e., all of the bonding orbital and antibonding orbital interactions between the bonds of the two units, in the NBO analysis. A negative value means that the interaction stabilizes the molecule. For both the gauche and trans transition states, E_{hyper} becomes more negative on going from X = F to Br. However, the magnitude of E_{hyper} of the trans transition state decreases faster than that of the gauche transition state. The net effect is that hyperconjugation energy difference between the two transition states (ΔE_{hyper}) increases from F to Br (Table

TABLE 5: Calculated Dipole Moments (μ , Debyes), C–C Bond Orders, C–C Bond Lengths (\AA), and Hyperconjugation Contributions (E_{hyper} , kJ mol^{-1}) of the Transition State ($\text{XCH}_2\text{CH}_2\cdots\text{H}\cdots\text{Y}$) of Reaction R1

X	Y	E_{hyper}^a			μ^b		bond order ^c		bond length ^b	
		trans	gauche	$\Delta E_{\text{hyper}}^d$	trans	gauche	trans	gauche	trans	gauche
F	F	-151.5	-149.4	2.2	1.511	2.202	1.030	1.033	1.505	1.502
Cl	F	-160.3	-157.2	3.1	1.764	2.405	1.034	1.033	1.507	1.506
Br	F	-167.2	-163.1	4.1	1.766	2.436	1.041	1.039	1.504	1.504
F	Cl	-156.9	-162.3	-5.4	1.127	4.105	1.031	1.043	1.498	1.490
Cl	Cl	-175.6	-170.1	5.5	1.138	4.016	1.046	1.043	1.491	1.493
Br	Cl	-193.1	-177.0	16.1	1.281	4.036	1.062	1.050	1.485	1.491
F	Br	-166.0	-169.0	-3.0	0.848	3.695	1.037	1.048	1.494	1.487
Cl	Br	-185.2	-177.4	7.8	0.816	3.652	1.053	1.047	1.486	1.489
Br	Br	-205.4	-186.7	18.7	0.847	3.724	1.073	1.054	1.478	1.487

^a NBO analysis, based on HF/6-31G(d)//MP2(full)/6-31G(d) wave function. ^b MP2/6-31G(d) values. ^c Wiberg bond order indices. ^d Difference between the gauche and trans transition states.

**Figure 2.** Partition scheme used in the NBO analysis of the transition states of reactions **R1** and **R2**.

5). This hyperconjugation interaction argument only fails to predict the ΔE_a value (-0.4 kJ mol^{-1}) for $X = Y = \text{F}$, where the energy of the gauche transition state is predicted to be higher than that of the trans transition state by 2.2 kJ mol^{-1} . A correlation plot between ΔE_a and ΔE_{hyper} shows an almost linear relationship ($R^2 = 0.95$; Figure 3). On the other hand, there is no apparent correlation between the difference in dipole moment and ΔE_a . These results clearly show that the hyperconjugation interaction is an important factor in determining the magnitude of ΔE_a .

Other properties which characterize the hyperconjugation interaction are the C–C bond length and bond order. The hyperconjugation interaction should lead to a shorter C–C bond and a larger C–C bond order in the transition state. As is evident in Figure 3, there are strong correlations between ΔE_a and the difference in C–C bond order as well as between ΔE_a and the difference in C–C bond length.

3.4. Rotational Barrier of the $\text{XCH}_2\text{CH}_2\cdot$ Radical with $X = \text{H}, \text{CH}_3, \text{F}, \text{Cl},$ and Br . For all of the $\text{XCH}_2\text{CH}_2\cdot$ radicals examined in this study, the ground-state structure favors an eclipsed conformation, where the C–X bond has an eclipsed arrangement with respect to the radical center (i.e., SOMO), whereas the transition state for C–C bond rotation has a perpendicular arrangement. As seen in Table 6, the calculated rotational barriers without ZPE correction for $X = \text{H}, \text{CH}_3,$ and F are all close to zero, and they have a negative barrier when ZPE correction is included. On the other hand, both $\text{ClCH}_2\text{CH}_2\cdot$ and $\text{BrCH}_2\text{CH}_2\cdot$ are predicted to have a significant rotational barrier, 5.0 and 10.7 kJ mol^{-1} (after ZPE correction), respectively. The rotational barriers of haloethyl radicals (i.e., $X = \text{F}, \text{Cl},$ and Br) have been studied recently by Zheng and Philips at the B3-LYP/6-311++G(3df,3pd) level.²⁶ Their calculated rotational barriers are $-2.5, 7.9,$ and 18.4 kJ mol^{-1} ,

for $X = \text{F}, \text{Cl},$ and Br , respectively. For the chlorine and bromine substituted systems, their calculated barriers are somewhat higher than our values. Our study confirms that the $\text{FCH}_2\text{CH}_2\cdot$ radical has a negligible rotational barrier. Therefore, we conclude that for $X = \text{H}, \text{CH}_3,$ and F the C–C bond rotation of the $\text{XCH}_2\text{CH}_2\cdot$ radical is free, whereas for $X = \text{Cl}$ and Br , the C–C rotation is hindered. This suggests that the configuration of β -fluorine substituted alkyl radicals and the unsubstituted alkyl radicals (represented by $X = \text{H}$ and CH_3) cannot be maintained during the abstraction reaction, whereas it is possible for β -chlorine and β -bromine substituted alkyl radicals.

Hoz et al. pointed out that for the $\text{XCH}_2\text{CH}_2\cdot$ radical, hyperconjugation interaction between the C–X bond and the C_α unpaired electron (in SOMO) of the radical center would stabilize the ground state.¹⁸ Hyperconjugation interaction is less important in the rotational transition state. As a consequence, there are significant differences between the equilibrium structure and transition state in the C–X and C–C bond lengths and the XCC angle (Table 7). The equilibrium structure is calculated to have a shorter C–C bond, a longer C–X bond, and a smaller XCC angle compared with the rotational transitional state. NBO analysis indicates that E_{hyper} increases on going from $X = \text{H}$ to Br for both the ground state and transition state (Table 6). However, E_{hyper} increases significantly faster for the ground state than the transition state. This leads to an overall increase of the hyperconjugation-interaction energy difference between the transition state and the ground state (designated as ΔE_{hyper}) from H to Br . It is worth noting that ΔE_{hyper} is larger than the corresponding rotational barrier. This suggests that other factors, such as steric and electrostatic effects, may also contribute to the overall rotational barrier. Unfortunately, the present population analysis schemes cannot accurately calculate these effects.^{44,45} Given the good correlation between the rotational barrier and ΔE_{hyper} , it is reasonable to conclude that hyperconjugation is the key contributing factor in determining the rotational barrier of the $\text{XCH}_2\text{CH}_2\cdot$ radical.

Based on DFT and LMP2 calculations, Goddard et al. predicted that the symmetrically bridged structure is the global energy minimum of the $\text{BrCH}_2\text{CH}_2\cdot$ radical.²⁴ However, we have shown in a very recent study⁶ that, although the bridged structure (2A_1) of bromoethyl radical corresponds to a stable equilibrium structure, it is 25.5 kJ mol^{-1} (G2(MP2,SVP)) less stable than the open structure. Similarly, we predict that the stable bridged chloroethyl radical is 45.4 kJ mol^{-1} (G2(MP2,SVP)) higher in energy than the open form.

3.5. Halogen Abstraction Reaction R2 with $X = \text{H}, \text{F}, \text{Cl},$ and Br and $Y = \text{F}, \text{Cl},$ and Br . The calculated barriers and enthalpies of the halogen abstraction reaction **R2** are given in Table 8. All halogen abstraction reactions are calculated to be

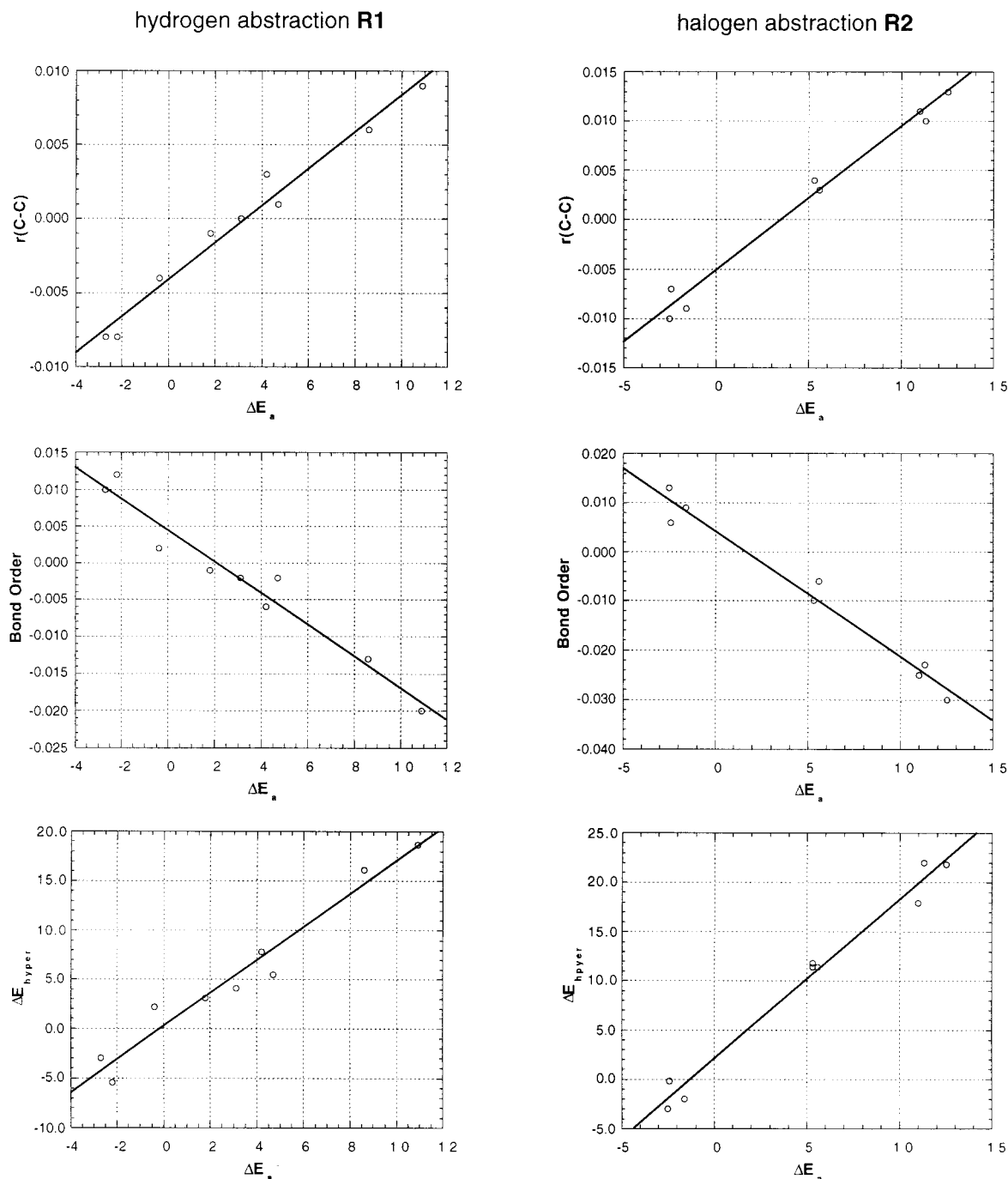


Figure 3. Correlation plots for the hydrogen abstraction reaction **R1** and halogen abstraction reaction **R2**.

TABLE 6: Calculated Rotational Barriers (kJ mol^{-1}) and Hyperconjugation Contributions (E_{hyper} , kJ mol^{-1}) of the $\text{XCH}_2\text{CH}_2\cdot$ Radical

X	rotational barrier ^a		E_{hyper} ^b	
	without ZPE	with ZPE	ground state	transition state
H	0.3	-1.0	-157.3	-156.6
CH ₃	0.1	-1.8	-163.3	-162.4
F	0.9	-2.0	-173.0	-167.1
Cl	8.5	5.0	-192.5	-174.1
Br	14.7	10.7	-212.3	-179.7

^a G2(MP2,SVP) values (include ZPE correction). ^b NBO analysis, based on HF/6-31G(d)/MP2(full)/6-31G(d) wave function.

exothermic, with the exothermicity decreases down the halogen group. As with reaction **R1**, the transition state of reaction **R2** is characterized by an almost linear $\text{C}\cdots\text{Y}\cdots\text{Y}$ framework

TABLE 7: Calculated Structural Parameters^a of the Ground State and Rotational Transition State (TS) of $\text{XCH}_2\text{CH}_2\cdot$ Radical

X	$r(\text{C}-\text{C})$		$r(\text{C}-\text{X})$		$\angle\text{XCC}$	
	ground state	TS	ground state	TS	ground state	TS
H	1.489	1.489	1.100	1.092	111.8	111.6
CH ₃	1.491	1.492	1.537	1.526	112.8	113.0
F	1.483	1.482	1.411	1.396	110.3	110.3
Cl	1.474	1.481	1.819	1.786	111.2	112.2
Br	1.462	1.484	2.009	1.959	110.0	111.9

^a MP2/6-31G(d) values.

(Figure 2). Interestingly, many of the halogenation abstraction reactions are calculated to have a negative energy barrier. This is due to the fact that the $\text{XCH}_2\text{CH}_2\cdot$ radical and halogen

TABLE 8: Calculated Barrier and Enthalpies (kJ mol⁻¹) of Reaction R2 (XCH₂CH₂• + Y₂ → XCH₂CH₂Y + Y•)

X	Y	barrier (E_a) ^b			enthalpy	
		trans	gauche	ΔE_a ^c	trans	gauche
H	F	22.9 (1.02)			-326.7	
F	F	27.1 (1.04)	24.7 (1.04)	-2.4	-321.3	-324.8
Cl	F	24.2 (1.04)	29.5 (1.04)	5.3	-321.4	-319.4
Br	F	24.9 (1.04)	35.9 (1.05)	11.0	-317.3	-312.8
H	Cl	-16.4 (0.85)			-118.6	
F	Cl	-8.4 (0.87)	-10.9 (0.87)	-2.5	-119.2	-117.2
Cl	Cl	-12.6 (0.87)	-7.0 (0.87)	5.6	-117.4	-112.7
Br	Cl	-12.3 (0.87)	-1.0 (0.87)	11.3	-112.1	-106.1
F	Br	-9.9 (0.84)	-11.5 (0.84)	-1.6	-101.8	-97.2
Cl	Br	-13.5 (0.84)	-8.1 (0.83)	5.3	-98.8	-92.7
Br	Br	-13.5 (0.85)	-1.0 (0.84)	12.5	-93.7	-85.6

^a G2(MP2,SVP) values (include ZPE correction). ^b The (S^2) values of the transition states are given in parentheses. ^c Difference between the barriers of gauche and trans abstractions.

TABLE 9: Calculated Energy Differences (ΔE_{gt} , kJ mol⁻¹), Hyperconjugation Contributions (E_{hyper} , kJ mol⁻¹), and Dipole Moments (μ , Debyes) of the gauche and trans Conformations of XCH₂CH₂Y

X	Y	ΔE_{gt} ^c	E_{hyper} ^a		μ^b	
			trans	gauche	trans	gauche
F	F	-3.50	-145.5	-156.2	0.000	3.064
Cl	F	1.98	-161.1	-162.7	0.136	3.169
Br	F	4.58	-169.6	-168.3	0.058	3.152
Cl	Cl	4.72	-173.7	-169.3	0.000	3.119
Cl	Br	6.03	-181.0	-175.0	0.091	3.074
Br	Br	8.16	-189.2	-182.2	0.000	3.017

^a NBO analysis, based on HF/6-31G(d)//MP2/6-31G(d) wave function. ^b MP2/6-31G(d) values. ^c Energy difference between the gauche and trans conformations; G2(MP2) values.

molecule (Y₂) readily forms a stable van der Waals complex, which is more stable than the transition state. However, the complex is just slightly more stable than the transition state, e.g., by 2 kJ mol⁻¹ for X = F and Y = Br. Thus, it is unlikely that the formation of a stable complex will influence the overall stereochemistry of reaction R2. A comparison of Tables 3 and 8 shows that for both reactions R1 and R2 the inductive effect of F, Cl, and Br increases the abstraction barrier compared with that for X = H. For the trans abstraction, the energy barrier first decreases from F to Cl and then increases slightly from Cl to Br for a given Y, whereas for the gauche abstraction, the energy barrier increases steadily from F to Br. For X = F, the gauche abstraction is favored in energy over the trans abstraction and vice versa for X = Cl and Br. This trend is similar to that of the hydrogen abstraction reaction R1. However, unlike reaction R1, the ΔE_a value of reaction R2 is almost the same for a given X.

Compared with reaction R1, the reaction enthalpies of R2 for the gauche and trans abstractions are not distinctly different. According to Polanyi–Evans relationship,⁴⁶ factors affecting the reaction enthalpy would also affect the energy barrier. Therefore, it would be instructive to determine the factors affecting the enthalpy difference between the two abstraction pathways, i.e., the energy difference between the gauche and the trans conformations of the product XCH₂CH₂Y.

The energy difference between the two conformations of XCH₂CH₂Y, their dipole moment, and E_{hyper} values are summarized in Table 9. The E_{hyper} term is also calculated by deleting all of the delocalization–interaction terms between the bonds on the two carbon atoms of the molecule. Except for 1,2-

difluoroethane (FCH₂CH₂F) which prefers a gauche conformation, all of the other systems prefer a trans rotamer. The unexpected gauche preference for the 1,2-disubstituted ethanes with the first-row substituent is the well-known gauche effect. Numerous theoretical studies have been reported on this gauche effect.^{47–53} The important factors which govern the energy difference between the gauche and trans conformations are polar, steric, and stereoelectronic effects.

Wolfe explained the gauche effect in terms of the attractive electron–nuclei interaction, the repulsive electron–electron and nuclei–nuclei interaction, and kinetic energy of electrons.^{47a} Basically, all of the interactions can be divided into attractive and repulsive terms. The dipole–dipole interaction is repulsive in the gauche conformation but attractive in the trans form. The steric effect is repulsive in both conformations but favors the trans conformation. The hyperconjugation interaction in both the gauche and trans conformations is attractive (energy lowering). The total effect is a combination of the three factors. If one employ the hyperconjugation interaction argument alone, the gauche conformation of FCH₂CH₂F and FCH₂CH₂Cl is predicted to be the preferred conformation. However, the trans conformation of FCH₂CH₂Cl is calculated to be more stable by the G2(MP2,SVP) theory. Because both the dipole–dipole interaction and the steric effect favor the trans conformation, it is the combined effect of these three factors that leads to a preference of the trans conformation in FCH₂CH₂Cl. Although the steric effect favors the trans conformation, its contribution is difficult to estimate. This is due to the fact that the atomic radius of the X atom increases from F to Br as well as the distance between X and Y also increases from F to Br for a given Y. Moreover, there is no apparent correlation between the energy difference and the difference in dipole moment. Because the hyperconjugation interaction correctly predicts the sequence of the energy differences between the gauche and trans conformations, it is safe to conclude that hyperconjugation is probably the major factor in determining the energy difference between the gauche and trans conformations of XCH₂CH₂Y.

The transition state of reaction R2 is analyzed in the same way as the transition state of reaction R1 and the XCH₂CH₂Y product. The dipole moments, C–C bond lengths, and E_{hyper} values of the transition state XCH₂CH₂•••Y•••Y are summarized in Table 10. As with XCH₂CH₂Y, both the dipole–dipole interaction and steric effect favor the trans transition state. However, their contributions should be smaller than those in the XCH₂CH₂Y systems, because the dipole moment difference between the gauche and trans transition states is smaller and also the X•••Y distance is longer compared with that in the XCH₂CH₂Y product. As seen in Table 10, the dipole moments of the gauche and trans transition states vary irregularly on going from X = F to Br for a given Y. The same is observed for the dipole-moment difference between the two transition states with Y = F and Br. There is no apparent correlation between the difference in dipole moment and the energy difference between the two transition states (ΔE_a).

The trend of ΔE_a can be explained in terms of hyperconjugation interaction. According to this argument, one predicts that the gauche transition state is lower in energy than the trans transition state for X = F, whereas for X = Cl and Br, the trans transition state is lower in energy. The C–C bond length and bond order, properties reflecting the strength of the hyperconjugation interaction, also indicate the same pattern as the hyperconjugation–interaction energy. In all cases, a strong correlation is found between ΔE_a and the properties characterizing the hyperconjugation interaction (Figure 3).

TABLE 10: Calculated Dipole Moments (μ , Debyes), C–C Bond Orders, C–C Bond Lengths (\AA), and Hyperconjugation Contributions (E_{hyper} , kJ mol^{-1}) of the Transition State ($\text{XCH}_2\text{CH}_2\cdots\text{Y}\cdots\text{Y}$) of Reaction **R2**

X	Y	E_{hyper}^a			μ^b		bond order ^c		bond length ^b	
		trans	gauche	$\Delta E_{\text{hyper}}^d$	trans	gauche	trans	gauche	trans	gauche
F	F	-173.0	-173.2	-0.2	1.123	2.549	1.045	1.051	1.488	1.480
Cl	F	-192.8	-181.4	11.4	1.290	2.678	1.058	1.048	1.479	1.483
Br	F	-211.0	-193.1	17.9	1.277	2.714	1.080	1.056	1.469	1.480
F	Cl	-169.3	-172.3	-3.0	0.599	3.721	1.039	1.052	1.492	1.482
Cl	Cl	-191.2	-179.8	11.4	0.557	3.632	1.057	1.051	1.481	1.484
Br	Cl	-210.5	-188.5	22.0	0.634	3.652	1.081	1.058	1.471	1.482
F	Br	-175.3	-177.2	-2.0	0.454	3.451	1.044	1.053	1.491	1.482
Cl	Br	-196.5	-184.7	11.8	0.463	3.331	1.062	1.052	1.480	1.484
Br	Br	-217.4	-195.6	21.8	0.382	3.400	1.088	1.059	1.469	1.481

^a NBO analysis, based on HF/6-31G(d)/MP2/6-31G(d) wave function. ^b MP2/6-31G(d) values. ^c Wiberg bond order indices. ^d Difference between the gauche and trans transition states.

3.6. Implication of Calculated Results on the Stereochemistry of Radical Halogenation of Alkanes and Alkenes. In the previous three sections, we have explained the patterns in the energy differences between the gauche and trans transition states of both reactions **R1** and **R2**, as well as the rotational barriers of the $\text{XCH}_2\text{CH}_2\cdot$ radicals in terms of hyperconjugation interaction. Here, we discuss the implication of our calculated results on the stereochemistry of radical halogenation of alkanes and alkenes.

For the hydrogen abstraction reaction **R1**, the X group vicinal to the reaction site could change the reactivity of the hydrogen atom at the reaction site and thus make the two hydrogen atoms at the gauche and trans positions diastereotopic.⁷ For X = F, the abstraction at the gauche position is slightly preferred, whereas for X = Cl and Br, the trans position is preferred. Hydrogen abstraction by Cl and Br at the trans position for X = Br is strongly preferred. The strong preference of the trans position for the Br atom was explained in terms of the anchimeric effect by Thaler.⁵⁴ Our calculations also predict that for X = F and Y = Cl and Br the gauche abstraction is slightly preferred in energy. To date, no direct experimental results can be found to support our prediction. Radical chlorination or bromination of fluorine substituted cycloalkanes can be used to prove our prediction. It is pertinent to note that these experiments may be difficult because the inductive effect of the F atom strongly disfavors the abstraction at the β position, as indicated in Table 3, and the abstraction barrier of the reaction **R1** with X = F is much higher than that with X = H.

The $\text{XCH}_2\text{CH}_2\cdot$ radical represents the product of the hydrogen abstraction reaction **R1** and the reactive intermediate in the halogenation of alkene. A high rotational barrier is required to maintain the radical configuration during the reaction and thus to give final stereoselective products (Figure 1). In addition, the subsequent halogen abstraction must be fast enough to ensure that the C–C bond rotation does not occur before the radical reacts with the halogen molecule (Y_2). In other words, the halogen abstraction barrier must be significantly lower than the corresponding rotational barrier. Our calculation results indicate that for X = H, CH_3 (represents an alkyl substituent), and F the C–C bond rotation is nearly free. Thus, the radical configuration cannot be maintained during the abstraction reaction. In addition, due to the significantly higher barrier of the reaction **R2** with Y = F (Table 8) compared with the rotational barrier of the $\text{XCH}_2\text{CH}_2\cdot$ radicals with X = Cl and Br (Table 6), the radical configuration of $\text{ClCH}_2\text{CH}_2\cdot$ and $\text{BrCH}_2\text{CH}_2\cdot$ cannot be retained during radical fluorination reaction. Thus, we predict that stereoselective products in the radical fluorination of alkanes and alkenes with unconstrained structure cannot be observed directly. However, it may be

observable under a condition which constrains the radical from undergo rotation, such as the use of the cyclic alkanes and alkenes.

The calculated results of chlorination and bromination are very different from that of fluorination. For the reaction of the $\text{XCH}_2\text{CH}_2\cdot$ radical with Cl_2 or Br_2 , the activation barrier is very low or even negative. In the case of X = F, Cl_2 and Br_2 prefer to attack the gauche position of the F atom. However, because of the facile C–C bond rotation of the $\text{FCH}_2\text{CH}_2\cdot$ radical, the gauche preference of radical chlorination and bromination of fluorine-substituted alkanes can only be observed for alkanes with constrained structure, such as cyclic alkanes. In distinct contrast, for X = Cl and Br, Cl_2 and Br_2 prefer to attack the gauche position of Cl or Br. These theoretical results are in excellent accord with experimental observations. For instance, Bellucci and Chiappe reported that in the radical bromination of 1,2-diphenylethylenes the gauche abstraction is preferred over the trans abstraction.⁵⁵

For radical chlorination and bromination, we found that the rotational barrier of the $\text{ClCH}_2\text{CH}_2\cdot$ radical is lower than that of the $\text{BrCH}_2\text{CH}_2\cdot$ radical, and for both reactions **R1** and **R2**, the trans abstraction is preferred in a larger extent with X = Br than with X = Cl. From these data, one can predict that for the radical chlorination and bromination of the chlorine substituted alkanes the reaction is less stereoselective compared with those of the bromine substituted alkanes. Similarly, radical chlorination of alkenes is less stereoselective than bromination. Again, our theoretical findings are in excellent accord with experimental results.^{2,3} For many years, the Skell hypothesis has been used to rationalize the stereospecificity of radical halogenations reactions.^{2–4,24} In this study, we show that it is not necessary to use the concept of “bridged” radical to explain the observed stereochemistry in radical halogenation.

4. Concluding Remarks

In this paper, we have studied the stereochemistry of radical halogenation of alkyl halides using the G2(MP2,SVP) method. For both reactions **R1** and **R2** with X = F, the abstraction prefers a gauche position of the F atom, whereas when X is Cl or Br, the abstraction prefers a trans position. The energy difference between the gauche and the trans transition state increases on going from X = F to Br for any given Y. Because of the almost free C–C bond rotation of the $\text{XCH}_2\text{CH}_2\cdot$ radical with X = H, CH_3 , and F, the halogenation of fluorine substituted alkanes and ordinary unsubstituted alkanes is predicted not to be stereoselective. The activation barrier of the fluorine abstraction reaction **R2** is significantly higher than the rotational barrier of the corresponding $\text{XCH}_2\text{CH}_2\cdot$ radical. Thus, although the

rotation of the $\text{ClCH}_2\text{CH}_2^*$ and $\text{BrCH}_2\text{CH}_2^*$ radicals is hindered, the radical fluorination of chlorine- or bromine-substituted alkanes with unconstrained structure is also predicted not to be stereoselective. On the contrary, chlorination and bromination of alkenes and chlorine- and bromine-substituted alkanes are calculated to be stereoselective. This is readily attributed to the trans preference of the hydrogen reaction **R1**, the hindered C—C bond rotation of the $\text{XCH}_2\text{CH}_2^*$ radical, and the low energy barrier and the trans preference of halogen abstraction **R2**. The stereochemical control in the radical halogenation reactions can be understood without the use of the Skell hypothesis. The trends in the calculated energy difference between the gauche and trans transition states of reactions **R1** and **R2**, the rotational barrier of $\text{XCH}_2\text{CH}_2^*$ radical, as well as the energy difference between the gauche and the trans conformations of $\text{XCH}_2\text{CH}_2\text{Y}$ can be explained in a uniform manner in terms of hyperconjugation interaction.

Acknowledgment. This work was supported by the National University of Singapore (Grant No. R-143-000-126-112) and the National Natural Science Foundation of China (Grant No. 29892167).

Supporting Information Available: Structural parameters (Table S1) and zero-point corrections (Table S2) related to reactions **R3** and **R4**. This material is available free of charge via the Internet at <http://pubs.acs.org>.

References and Notes

- (1) Skell, P. S.; Tuleen, D. L.; Readio, P. D. *J. Am. Chem. Soc.* **1963**, *85*, 2849.
- (2) Skell, P. S.; Shea, K. J. In *Free Radicals Vol. 2*; Kochi, J. K., Ed.; Wiley: New York, 1973; Chapter 26.
- (3) Walling, C. In *Molecular Rearrangements Vol. 1*; de Mayo, P., Ed.; Wiley: New York, 1963; Chapter 7.
- (4) Skell, P. S.; Traynham, J. G. *Acc. Chem. Res.* **1984**, *17*, 160.
- (5) (a) Engels, B.; Peyerimhoff, S. D. *J. Mol. Struct. (THEOCHEM)* **1986**, *138*, 59. (b) Engels, B.; Peyerimhoff, S. D. *J. Phys. Chem.* **1989**, *93*, 4462. (c) Engels, B.; Peyerimhoff, S. D.; Skell, P. S. *J. Phys. Chem.* **1990**, *94*, 1267.
- (6) Li, Z.-H.; Fan, K.-N.; Wong, M. W. *J. Org. Chem.* Submitted for publication.
- (7) (a) Sicher, J.; Závada, J. *Collect. Czech. Commun.* **1967**, *66*. (b) Sicher, J.; Závada, J.; Pánková, M. *Collect. Czech. Commun.* **1968**, 1147.
- (8) Pasto, D. J.; Krasnansky, R.; Zercher, C. *J. Org. Chem.* **1987**, *52*, 3062.
- (9) (a) Hoffmann, R.; Radom, L.; Pople, J. A.; Schleyer, P. v. R.; Hehre, W. J.; Salem, L. *J. Am. Chem. Soc.* **1972**, *94*, 6221. (b) Radom, L.; Paviot, J.; Pople, J. A. *J. Chem. Soc., Chem. Commun.* **1974**, 58. (c) Pross, A.; Radom, L. *Tetrahedron* **1980**, *36*, 1999. (d) Saebo, S.; Beckwith, A. L. J.; Radom, L. *J. Am. Chem. Soc.* **1984**, *106*, 5119.
- (10) (a) Schlegel, H. B. *J. Phys. Chem.* **1982**, *86*, 4678. (b) Schlegel, H. B.; Sosa, C. *J. Phys. Chem.* **1984**, *88*, 1141.
- (11) Hopkinson, A. C.; Lien, M. H.; Csizmadia, I. G. *Chem. Phys. Lett.* **1980**, *71*, 557.
- (12) Biddles, I.; Hudson, A. *Chem. Phys. Lett.* **1973**, *18*, 45.
- (13) Fossey, J.; Nedelec, J.-Y. *Tetrahedron* **1981**, *37*, 2967.
- (14) Kato, S.; Morokuma, K. *J. Chem. Phys.* **1980**, *72*, 206.
- (15) (a) Zipse, H. *J. Chem. Soc., Perkin Trans. 2* **1996**, 1797. (b) Zipse, H. *J. Am. Chem. Soc.* **1997**, *119*, 1087. (c) Zipse, H. *J. Am. Chem. Soc.* **1997**, *119*, 2889.
- (16) Harding, B. L. *J. Am. Chem. Soc.* **1981**, *103*, 7469.
- (17) Russell, J. J.; Rzepa, H. S.; Widdowson, D. A. *J. Chem. Soc., Chem. Commun.* **1983**, 625.
- (18) Hoz, T.; Sprecher, M.; Basch, H. *J. Phys. Chem.* **1985**, *89*, 1664.
- (19) (a) Guerra, M. *Chem. Phys. Lett.* **1987**, *139*, 463. (b) Guerra, M. *J. Am. Chem. Soc.* **1992**, *114*, 2077.
- (20) Clark, T.; Symons, M. C. R. *J. Chem. Soc., Chem. Commun.* **1986**, 96.
- (21) Molino, L. M.; Poblet, J. M.; Canadell, E. *J. Chem. Soc., Perkin Trans. 2* **1982**, 1217.
- (22) (a) Bernardi, F.; Bottoni, A.; Fossey, J.; Sorba, J. *J. Mol. Struct.* **1985**, *119*, 231. (b) Bernardi, F.; Bottoni, A.; Fossey, J.; Sorba, J. *Tetrahedron* **1986**, *42*, 5567. (c) Bernardi, F.; Fossey, J. *J. Mol. Struct.* **1988**, *180*, 79.
- (23) (a) Chen, Y.; Rauk, A.; Tschuikow-Roux, E. *J. Chem. Phys.* **1990**, *93*, 6620. (b) Chen, Y.; Tschuikow-Roux, E. *J. Phys. Chem.* **1992**, *96*, 7266.
- (24) Ihee, H.; Zewail, A. H.; Goddard, W. A., III. *J. Phys. Chem. A* **1999**, *103*, 6638.
- (25) (a) Sekusak, S.; Gusten, H.; Sabljic, A. *J. Phys. Chem.* **1996**, *100*, 6212. (b) Sekusak, S.; Liedl, K. R.; Rode, B. M.; Sabljic, A. *J. Phys. Chem. A* **1997**, *101*, 4245. (c) Sekusak, S.; Sabljic, A. *Chem. Phys. Lett.* **1997**, *272*, 353. (d) Sekusak, S.; Bartlett, R. J.; Sabljic, A. *J. Phys. Chem. A* **1999**, *103*, 11394.
- (26) Zheng, X.; Phillips, D. L. *J. Phys. Chem. A* **2000**, *104*, 1030.
- (27) Martell, J. M.; Boyd, R. J. *J. Phys. Chem.* **1995**, *99*, 13402.
- (28) (a) Talhaoui, A.; Louis, F.; Devolder, P.; Meriaux, B.; Sawerysyn, J.-P.; Rayez, M. T.; Rayez, J. C. *J. Phys. Chem.* **1996**, *100*, 13531. (b) Louis, F.; Talhaoui, A.; Sawerysyn, J.-P.; Rayez, M. T.; Rayez, J. C. *J. Phys. Chem. A* **1997**, *101*, 8503.
- (29) Chandra, A. K.; Uchimaru, T. *J. Phys. Chem. A* **1999**, *103*, 10874.
- (30) Seetula, J. A. *J. Chem. Soc., Faraday Trans.* **1998**, *94*, 3561.
- (31) Frisch, M. J.; Trucks, G. W.; Schlegel, H. B.; Scuseria, G. E.; Robb, M. A.; Cheeseman, J. R.; Zakrzewski, V. G.; Montgomery, J. A., Jr.; Stratmann, R. E.; Burant, J. C.; Dapprich, S.; Millam, J. M.; Daniels, A. D.; Kudin, K. N.; Strain, M. C.; Farkas, O.; Tomasi, J.; Barone, V.; Cossi, M.; Cammi, R.; Mennucci, B.; Pomelli, C.; Adamo, C.; Clifford, S.; Ochterski, J.; Petersson, G. A.; Ayala, P. Y.; Cui, Q.; Morokuma, K.; Malick, D. K.; Rabuck, A. D.; Raghavachari, K.; Foresman, J. B.; Cioslowski, J.; Ortiz, J. V.; Stefanov, B. B.; Liu, G.; Liashenko, A.; Piskorz, P.; Komaromi, I.; Gomperts, R.; Martin, R. L.; Fox, D. J.; Keith, T.; Al-Laham, M. A.; Peng, C. Y.; Nanayakkara, A.; Gonzalez, C.; Challacombe, M.; Gill, P. M. W.; Johnson, B. G.; Chen, W.; Wong, M. W.; Andres, J. L.; Head-Gordon, M.; Replogle, E. S.; Pople, J. A. *Gaussian 98*, revision A.2; Gaussian, Inc.: Pittsburgh, PA, 1998.
- (32) Curtiss, L. A.; Redfern, P. C.; Smith, B. J.; Radom, L. *J. Chem. Phys.* **1996**, *104*, 5148.
- (33) Curtiss, L. A.; Raghavachari, K.; Trucks, G. W.; Pople, J. A. *J. Chem. Phys.* **1991**, *94*, 7221.
- (34) Curtiss, L. A.; Redfern, P. C.; Raghavachari, K.; Rassolov, V.; Pople, J. A. *J. Chem. Phys.* **1999**, *110*, 4703.
- (35) For example, see: Montgomery, J. A., Jr.; Frisch, M. J.; Ochterski, J. W.; Petersson, G. A. *J. Chem. Phys.* **1999**, *110*, 2822.
- (36) (a) Becke, A. D. *J. Chem. Phys.* **1993**, *98*, 5648. (b) Lee, C.; Yang, W.; Parr, R. G. *Phys. Rev. B* **1988**, *37*, 785.
- (37) Jensen, F. *Chem. Phys. Lett.* **1990**, *169*, 519.
- (38) Mayer, P. M.; Parkinson, C. J.; Smith, D. M.; Radom, L. *J. Chem. Phys.* **1998**, *108*, 604.
- (39) Wong, M. W.; Radom, L. *J. Phys. Chem. A* **1998**, *102*, 2237.
- (40) (a) Scott, A. P.; Radom, L. *J. Phys. Chem.* **1996**, *100*, 16502. (b) Pople, J. A.; Scott, A. P.; Wong, M. W.; Radom, L. *Isr. J. Chem. Soc.* **1993**, *33*, 345.
- (41) Denisov, E. In *General Aspects of the Chemistry of Radicals*; Alfassi, Z. B., Ed.; Wiley: Chichester, U.K., 1999; Chapter 4 and references therein.
- (42) Wiberg, K. B. *Tetrahedron* **1968**, *24*, 1083.
- (43) (a) Foster, J. P.; Weinhold, F. *J. Am. Chem. Soc.* **1980**, *102*, 7211. (b) Reed, A. E.; Weinhold, F. *J. Chem. Phys.* **1983**, *78*, 4066. (c) Reed, A. E.; Weinstock, R. B.; Weinhold, F. *J. Chem. Phys.* **1985**, *83*, 735. (d) Reed, A. E.; Weinhold, F. *J. Chem. Phys.* **1985**, *83*, 1736.
- (44) (a) Badenhoop, J. K.; Weighold, F. *J. Chem. Phys.* **1997**, *107*, 5406. (b) Badenhoop, J. K.; Weighold, F. *Int. J. Quantum Chem.* **1999**, *72*, 269.
- (45) Goodman, L.; Gu, H.; Pophristic, V. *J. Chem. Phys.* **1999**, *110*, 4268.
- (46) Evans, M. G.; Polanyi, M. *Trans Faraday Soc.* **1938**, *34*, 11.
- (47) (a) Wolfe, S. *Acc. Chem. Res.* **1972**, *5*, 102. (b) Pinto, B. M.; Schlegel, H. B.; Wolfe, S. *Can. J. Chem.* **1987**, *65*, 1658.
- (48) Thibaudeau, C.; Plavec, J.; Garg, N.; Papchikhin, A.; Chattopadhyaya, J. *J. Am. Chem. Soc.* **1994**, *116*, 4038.
- (49) (a) Wiberg, K. B.; Murcko, M. A.; Laidig, K. E.; Macdougall, P. *J. Phys. Chem.* **1990**, *94*, 6956. (b) Wiberg, K. B. *Acc. Chem. Res.* **1996**, *29*, 229.
- (50) Rablen, P. R.; Hoffmann, R. W.; Hrovat, D. A.; Borden, W. T. *J. Chem. Soc., Perkin Trans. 2* **1999**, *8*, 1719.
- (51) Craig, N. C.; Chen, A.; Suh, K. H.; Klee, S.; Mellau, G. C.; Winnewisser, B. P.; Winnewisser, M. *J. Am. Chem. Soc.* **1997**, *119*, 4789.
- (52) Engkvist, O.; Karlstrom, G.; Widmark, P. O. *Chem. Phys. Lett.* **1997**, *265*, 19.
- (53) (a) Senderowitz, H.; Fuchs, B. *Tetrahedron* **1994**, *50*, 9707. (b) Senderowitz, H.; Fuchs, B. *J. Mol. Struct. Theochem.* **1997**, *395*, 123. (c) Wong, M. W.; Wiberg, K. B.; Frisch, M. J. *J. Comput. Chem.* **1995**, *16*, 385.
- (54) Thaler, W. A. *J. Am. Chem. Soc.* **1963**, *85*, 2607.
- (55) Bellucci, G.; Chiappe, C. *J. Phys. Org. Chem.* **1998**, *11*, 685.